PNAS RESEARCH ARTICLE | APPLIED PHYSICAL SCIENCES OPEN ACCESS

Geometric modeling of knitted fabrics

Lauren Niu[a,b], Geneviève Dion[a], and Randall D. Kamien[b,1]

Edited by John Rogers, Northwestern University–Evanston, Evanston, Illinois; received August 15, 2024; accepted December 24, 2024

Knitting can turn a one-dimensional yarn into a highly ramified three-dimensional structure. As a method of additive manufacturing, it holds promise for a class of lightweight, ultrastrong materials. Here, we present a purely geometric model to predict the three-dimensional self-folding of knitted fabrics made only of the two traditional stitches, knit and purl.

geometry | origami | knitting | textile

Significance

Through a sequence of moves on a one-dimensional strand, knitting creates complex, self-folding, three-dimensional structures. The general geometric motifs that arise are independent of the particular yarns that are used, whether they are elastic, natural, or synthetic. By using the theory of thin shells in the "thick-shell" regime, we are able to capture the folding patterns of a wide variety knitted patterns composed only of the simple stitches, knit and purl. Moreover, the folding pattern is weakly dependent on the parameters of the energetic model, consistent with the observation that folding is generic.

It is undeniable that, by any metric, geometry plays a central role in our understanding of the physical world. From celestial mechanics (1) to soap bubbles (2) and from optics (3) to gravity (4), the rigor of geometric logic intoxicates our thinking. Indeed, because of their intrinsic elegance and potential application, tools have been developed to make materials that assemble into a targeted topography. Whether it be through the techniques of origami (5–7), thermal activation of local material anisotropy (8), or pneumatic actuation (9), the common thread is the use of isometric or near-isometric embeddings. Knit materials, on the other hand, have relatively small elastic moduli and can be designed by their creator to fold into complex three-dimensional patterns upon their construction, even without material postprocessing. Here, we propose a purely geometric model that can rationalize the folding of a myriad of knit motifs, and provide direct qualitative comparison between our simulated results and knitted fabrics.

Self-Folding Knits. Weft-knit materials showcase a wide variety of complex geometric and mechanical behavior (10–14). The three-dimensional (3D) structure of these patterns typically requires no or minimal postprocessing after initial fabrication, and their forms are robust to extensive handling in a variety of environments. Although the exact 3D form generated from a knit pattern may differ based on the choice of yarn and other fabrication parameters, the qualitative form does not depend on these parameters; knitted swatches created at a wide variety of length scales and moduli form similar buckling patterns. Although the focus of our study is on planar weft-knitted fabrics as shown in Fig. 1*A*, changing the topology of the whole fabric can yield a variety of different structures with large-scale 3D properties (Fig. 1*B*).

The basic stitch of a weft-knitted fabric is shown in Fig. 2*A* and is formed by drawing a loop of yarn through a previously existing loop. When the drawn yarn is pulled from "back to front" through the previous loop, the resulting stitch is called a knit stitch; a loop of yarn drawn through from "front to back" creates a purl stitch. The structure of knit and purl stitches differ only by a 180° rotation, which flips the orientation of crossings in a diagram of the yarn path. The back side of a fabric created with knit stitches is therefore functionally identical to the front side of a fabric created with purl stitches.

This local topological structure of knit and purl stitches, dictated at fabrication, creates the overall tendency for a knitted swatch to curl dramatically (Fig. 2*A*) (15, 16). This preferred "natural" curvature appears to be primarily a bulk phenomenon since the free boundaries of a knit swatch develop large curvatures regardless of their positions (Fig. 2 *B* and *C*). The top and bottom edges of knit swatches tend to curl forward, while the sides curl backward; purl swatches do exactly the opposite (Fig. 2*A*).

From Yarn Topology to Fabric Geometry. The preferred, natural curvatures of a knit or purl fabric can be estimated from the orientation of its yarn crossings in the plane and the resulting bending moments. At any given crossing, the two roughly perpendicular yarns must curve over or under each other, requiring them to bend out of the fabric plane (Fig. 2*D*). For any yarn with nonzero flexural modulus, this creates a bending moment in the opposite direction. This results in nonzero bending moments at the yarn crossing along the directions of both the *Top* yarn and the *Bottom* yarn, with opposite signs for each. In a region of knit (purl) stitches, all of the crossings align in a similar direction such that the *Top* (*Bottom*) yarn is roughly vertical and the *Bottom* (*Top*) yarn is roughly

Author affiliations: [a]Center for Functional Fabrics, Drexel University, Philadelphia, PA 19104; and [b]Department of Physics and Astronomy, University of Pennsylvania, Philadelphia, PA 19104

Author contributions: L.N., G.D., and R.D.K. designed research; L.N., G.D., and R.D.K. performed research; L.N., G.D., and R.D.K. analyzed data; G.D. contributed material samples; L.N. generated the necessary computer code; and L.N., G.D., and R.D.K. wrote the paper.

The authors declare no competing interest.

This article is a PNAS Direct Submission.

[1]To whom correspondence may be addressed. Email: kamien@upenn.edu.

Published February 11, 2025.

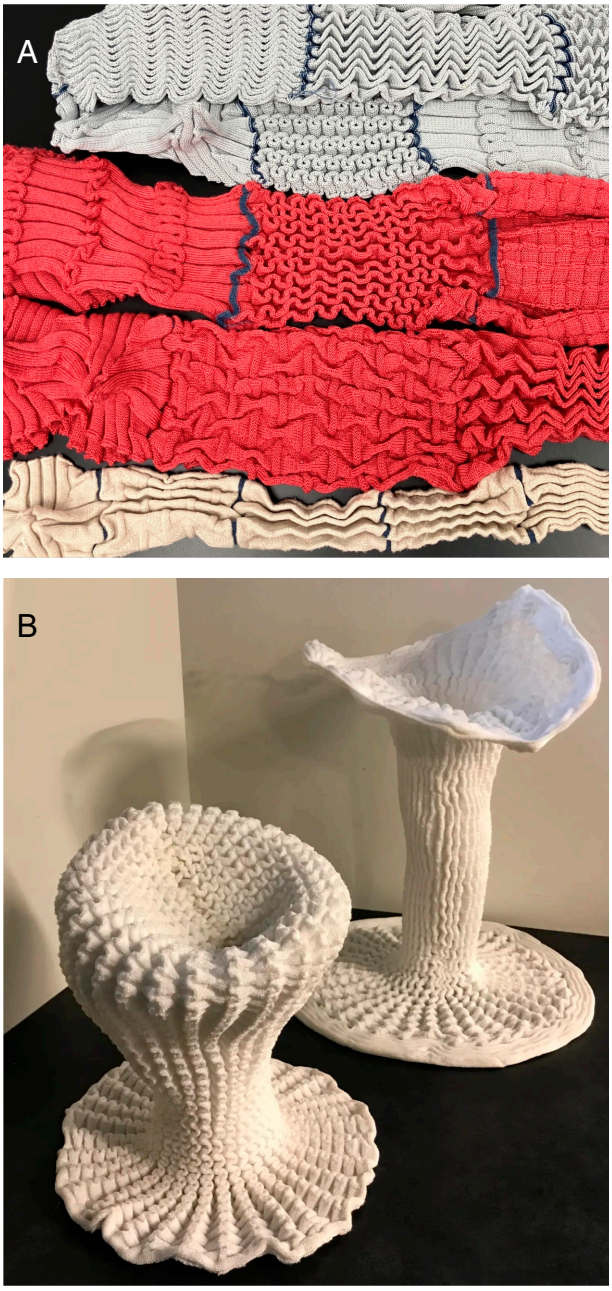

Fig. 1. (*A*) Samples of periodic self-folding weft knit patterns, knitted by machine from three different types of yarn. From *Top* to *Bottom*: recycled REPREVE® nylon yarn, Jaguar Modal/Nylon yarn, and Ecocot cotton yarn. (*B*) Weft knits with stitch patterns that have nonflat topology (*Left*: elliptical, *Right*: cylindrical) can also be used to shape large 3D forms. Samples were knitted with a nylon/PET blended yarn and steamed after fabrication to rigidify the fabric. Figure reproduced with permission from ref. 22.

horizontal (Fig. 2*A*). This results in a field of aligned bending moments, which drives the observed curvatures and buckling behavior of the fabric.

Most weft-knitted fabrics, whether produced by machine or by hand, are created while keeping consistent tension on the yarn, and typically with the goal of maintaining an even stitch size. We therefore assume that the length of each knitted loop remains roughly the same across the entire fabric and therefore that the "area" of a knitted stitch does not vary significantly over a swatch of 100 or more stitches. Additionally, yarn loops in the final fabric tend to fill space, leaving minimal gaps in the overall material; accordingly, distorting the lengths of knit or purl stitches postfabrication requires overcoming a significant amount of yarn-to-yarn friction (17–19).

The even stitch size, coupled with the condition that we only study flat knit–purl patterns with no topological pattern defects [such as short rows or increases/decreases between rows (20, 21)], suggests that our final fabrics should have a near-flat metric, even in their self-folded state. We can then invoke Gauss's celebrated *Theorema Egregium*, which states that, for an initially flat surface, deformations in three dimensions with nonzero Gaussian curvature (simultaneous curvature in multiple directions, resembling a saddle surface or a spherical dome or bowl) require some regions of the surface to stretch or compress tangentially. Because stretching or compressing a knitted fabric tangentially requires distorting the shape of stitch loops, we expect that the equilibrium configurations of a knitted swatch will naturally minimize observed regions of large Gaussian curvature. The result is that rectangular swatches of knit or purl stitches tend to curl cylindrically, which requires no Gaussian curvature, or remain nearly flat (Fig. 2*A*). Gaussian curvature may still appear in the final surface, albeit at an energetic cost. To be precise, in *Materials and Methods*, we denote the preferred, flat metric as a_0 and the mechanically preferred curvature tensor as b_0. The observed metric and curvature tensors of the deformed surface are denoted as a and b, respectively, and are, due to Gauss, not completely independent. The final structure is an energetic compromise between stretching (arising from the difference between a and a_0) and bending (between b and b_0) contributions. Note that the a_0 and b_0 need not satisfy the Theorem and are, therefore, independent.

Two-Dimensional Surface Approximation. Our observations of the physical samples suggest that we can approximate the buckled shape of an arbitrary rectangular knit and purl patterns as an elastic sheet with nonzero bending and stretching moduli, imbued with a field of preferred natural curvatures matching the knit/purl pattern. For simplicity, we use an elastic model implementing a Föppl–von-Kármán energy for thin shells with two-dimensional stretching and bending contributions. As minimizing this energy requires solving a global optimization problem that is analytically intractable for our patterns, we use a finite-difference simulation to compare our results with machine-knitted samples.

Because the structure of a knitted swatch differs significantly from the structure of an isotropic elastic sheet, we do not expect the details of the elastic formulation to significantly affect the results. In particular, we do not expect the elastic thickness parameter h used in our simulations to coincide with the physical thickness t of a knitted fabric, although we expect them to be at similar order. Rather, h remains a free tuning parameter that relates the effective bending stiffness of the fabric to its in-plane tensile stiffness. We also note that the physical bending stiffness of a physical knitted fabric may vary based on the stitch patterning and fabrication parameters.

As the elastic sheet approximation by definition ignores the structure of features below the length scale of h, which in our case is comparable to the dimensions of a single stitch, we ignore corrections to the elastic sheet energy beyond second order in the in-plane strain or out-of-plane curvature.

From experimental observations in Fig. 2 *A*–*C*, small swatches of knit materials with dimensions of approximately 40 stitches per side length show large natural curvatures both in the vertical and horizontal directions. We do not measure these natural curvatures physically, but we note that all free boundaries of fully knit or fully purl samples naturally rolled up tightly enough that their

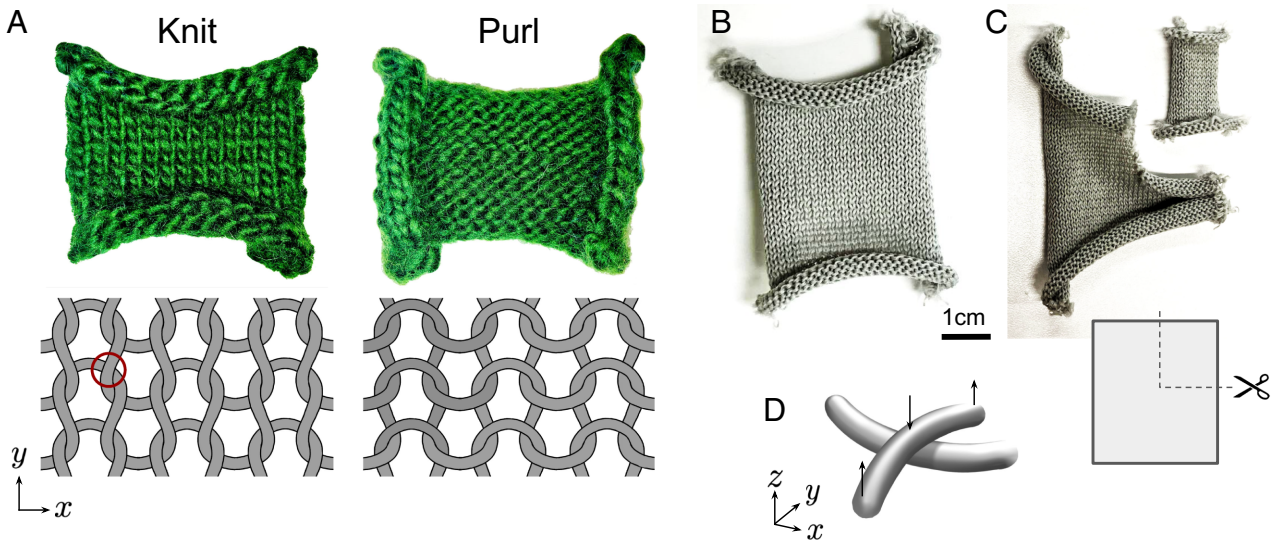

Fig. 2. (*A*) Two merino wool swatches made entirely from knit stitches and purl stitches (*Top*), and their yarn crossing diagrams (*Bottom*). These swatches exhibit curvature in multiple directions; the knit swatch curls forward at the *Top* and *Bottom* edges, and backward at the sides, while the purl swatch curls in the opposite directions. A yarn crossing, circled in red, requires yarns to cross-over/under each other in the plane (Fig. 2*D*). (*B*) A small rectangular piece cut from a larger knit swatch (REPREVE® nylon yarn, approximately 0.5mm diameter) displays the same rolling behavior as in (*A*). (*C*) When a corner of the knit swatch in (*B*) is cut away (schematic shown below), all free boundaries continue to curl significantly. This implies that the edge curling behavior observed in knit swatches is likely due to a bulk rather than a boundary stress. (*D*) At any yarn crossing in a textile, e.g. as highlighted in Fig. 2*A*, the two strands must bend around each other to avoid physically intersecting. Two initially straight yarns aligned with the *x* and *y* axes experience reaction bending moments that are positive along the *y*-direction (*Top* yarn) and negative along the *x*-direction (*Bottom* yarn). Arrows denote the corresponding local forces on the *Top* yarn. The field of bending moments generated from each yarn crossing contributes to the overall geometry of the fabric.

curvatures were limited by self-intersection of the fabric, such that $|\kappa|_x \sim |\kappa|_y \sim 1/t$, where t is the thickness of the fabric.

Results

Fig. 3 shows a comparison of several numerical computations of fabric self-folding (all with identical parameters) alongside experimental swatches knitted from nylon REPREVE® yarn using the same patterns. We use a quasistatic method for simulation to grow the patterns, starting from a flat sheet and incrementally increasing the magnitudes of κ_x and κ_y at every step, using each step's solution as the initial condition for the following step—you have to grow wefts to fold them. Further details about the knitting process and simulation setup are given in *Materials and Methods*.

We include simulations of several knit–purl patterns that are "unbalanced," with a larger total density of either knit or purl stitches (Fig. 3 *B*, *C*, *F*, and *G*). This imbalance results in observed out-of-plane curvatures at scales comparable to (if not larger than) the length scale of the pattern's features. For these cases, we included a set of weak springs in the simulation that connect the mesh's boundary vertices to their initial planar positions, keeping the fabric relatively flat overall and allowing us to emphasize the smaller-scale patterning. Physical samples do sometimes allow for these large-scale observed curvatures, although for our samples these features were largely mitigated when simply placed on a table or allowed to hang under gravity.

Tuning Parameters. In our simulations, we chose natural curvatures κ_x and κ_y smaller than the inverse thickness $1/h$ to avoid generating deformations large enough to cause the surface to self-intersect, as our simulation does not penalize self-intersecting surfaces. We also note that self-avoidance forces may be critical to the formation of certain knit–purl buckling patterns in a fully relaxed fabric. Although we used $|\kappa_x| = |\kappa_y|$ for simplicity in our model, we expect experimentally that $|\kappa_x| \neq |\kappa_y|$ as the knit structure (Fig. 2*A*) is inherently anisotropic.

As noted previously, the elastic sheet thickness h (set to 0.5 for all simulations in Fig. 3) serves as a tuning parameter relating the fabric's effective bending and tensile moduli, and a suitable value was chosen based on comparisons between initial simulations and experiment. In particular, smaller values of h energetically disfavor regions of nonzero Gaussian curvature, which appear in localized regions of knitted patterns. Indeed, for patterns with curved ridges (e.g. Fig. 3 *A* and *E*), too-small values of h ($h = 0.1$ in our case) fail to recapitulate such features; however, increasing the value of h up to 1.0 did not affect the patterning.

Finally, we note that swatches of pure knit or purl stitches show the Poisson effect, implying $0 < \nu < 0.5$, where ν is the 3D Poisson ratio of the material (12). In our simulations, we chose $\nu = 0.4$ to approximate the material as having a small amount of compressibility, but variations of ν between 0 and 0.5 have no significant visual effect. The buckling patterns generated in Fig. 3 are generic and not strongly dependent on the exact parameters h, $\kappa_x = \kappa_y$, and ν. Because of the computational cost, we have not done an exhaustive study of the parameter space on all patterns shown in Fig. 3: Changes in these values (of up to 50%) did not affect the folding pattern.

Discussion

The problem of designing a self-folding knitted swatch is distinct from the problem of designing folding patterns for traditional origami. In particular, interfaces between regions of knit and purl stitches often do not correspond to regions of large fabric curvatures or folds, and the "creases" observed in a self-folding knitted fabric may be difficult to guess simply by looking at the stitch pattern itself. Because the natural curvatures κ_x and κ_y change sign at any knit–purl interface, these interfacial regions typically remain flat. For instance, in the Miura-Ori

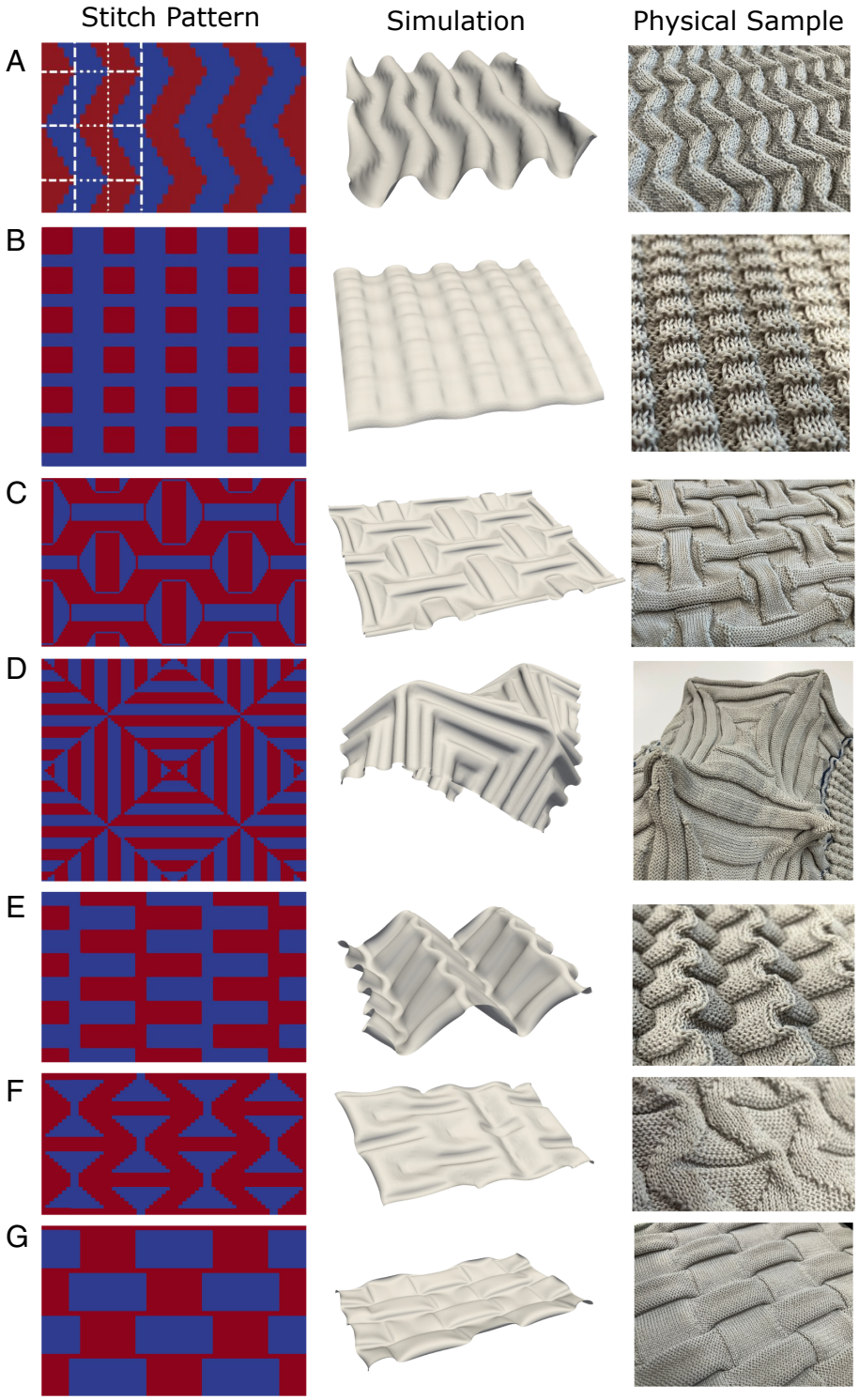

Fig. 3. (*A*–*G*) Comparison of knit–purl patterns (*Left*), simulated meshes (center), and knitted samples (*Right*). Red regions represent knit stitches; blue regions represent purl stitches. Note that not all patterns are at the same scale or have the same number of stitches. Parameters for all simulations are as follows: Each rectangular "stitch" in the mesh has dimension 1.4×1.2 (based on the stitch aspect ratio from knit samples). The elastic thickness parameter $h = 0.5$, and material parameters for the (isotropic) elastic surface approximation are Young's modulus $Y = 1$ and Poisson ratio $\nu = 0.4$. Natural curvatures $\kappa_x = -1$, $\kappa_y = 1$ are used for knit regions and $\kappa_x = 1$, $\kappa_y = -1$ for purl regions. Pattern in (*A*) has some fold lines overlaid on the *Left* side to show the crease pattern in the final fabric. Dashed lines represent valley folds; dotted lines represent mountain folds. Patterns in (*B*, *C*, *F*, and *G*) are not symmetric with respect to the density of knit and purl stitches, and with free boundary conditions, the meshes will develop curvature at large wavelengths. To mitigate this effect, we use weak springs at boundary vertices with spring constant per unit length 10^{-4} between the vertices and their positions on the initial (flat) mesh. Boundary conditions are otherwise all free. All experimental samples, besides (*D*), are slightly stretched in the fabric plane to emphasize their texture near the flat state, and to avoid the amount of self-intersection relevant to the pattern. Simulations did not forbid self-intersection.

knitting pattern (Fig. 3*A*) the observed "fold lines" run directly horizontally and vertically instead of following the diagonal interfaces between knit and purl stitches that one might expect from the origami structure (23).

The final form of the fabric is not in general locally predictable, as its shape is the result of solving a global optimization problem. Therefore, even patterns that are visually similar may yield dramatically different fabric textures. However, we note that all sharp creases and regions of large curvature tend to be cylindrical and aligned either horizontally or vertically, and they follow the axis-aligned principal curvature directions of plain knit or purl swatches. Locally, we can thus view each knit region of the fabric (on the order of a few stitch lengths) as being selected to curl cylindrically in the x direction (negatively), y direction (positively), or remain flat. A purl region of the fabric has similar choices, with opposite curvatures.

Future Improvements. Although the goal of our analysis is simply to reproduce the initial buckling pattern of fabrics made with knit and purl stitches, several improvements could be made that we have so far ignored in favor of simplicity and parsimony in the initial model.

Fig. 3 *A*, *E*, and *F* show the tendency for some knit–purl patterns to form sharp creases or corners, with features at length scales comparable to single stitches and the thickness of the fabric. Although we approximate knitted stitches as having no internal structure, such creases emerge frequently in knits. However, simulation of such features likely depends on the geometry of individual stitches, and furthermore requires, for instance, discretizing the mesh on scales much smaller than the thickness or parameterizing the yarn path within the stitch itself (16), which becomes computationally costly and fails to capture the obvious variation of the yarn at that scale.

Furthermore, regions of knit and purl stitches meeting at a horizontal or vertical interface are offset slightly relative to each other (in the direction normal to the fabric plane), and these offset features remain even when the fabric is flattened under tension. These offsets are typically at the stitch length scale, but we note that they might have effects on the equilibrium fabric shape and its mechanics. In particular, across these offsets the physical fabric thickness is not well-defined, and the effective bending moduli of these regions may be significantly different from those within a bulk region of knit or purl stitches.

We assumed isotropic elasticity in our model as well as constant thickness and moduli throughout the material. Even swatches made from purely knit stitches are anisotropic in their moduli, and as mentioned other physical moduli need not be assumed homogeneous, particularly across a knit–purl boundary (24, 25). However, our choice of model was partially motivated by the desire to find as simplistic a description as possible of patterning in knit–purl motifs.

Finally, we hope to include an energetic cost to the fabric's self-intersection in future work. We hope that this work acts as a catalyst for the science of Knitogami™.

Conclusion. We have shown that a simple approximation of planar knit–purl patterns as elastic sheets, with natural curvatures defined according to the stitch pattern, can recapitulate the self-folding behavior of several knit–purl motifs. Although the model does not capture quantitative details of the knitted fabric at the stitch length scale, it shows promise in helping to design complex patterns with simple knit structures, as well as motivating a simple framework for understanding knitted fabric geometry.

Materials and Methods

Experimental Samples. All fabric samples used for comparison with simulation were knitted using Unifi REPREVE® Performance nylon yarn (doubled), on a Shima Seiki SSG 122SV two-bed weft knitting machine.

Two-Dimensional Surface Simulation. When we observe the folded fabric we find that the general geometric motifs are independent of the details of the yarn and machine parameters. With this in mind, we do not expect it to be necessary to provide the specific details of the two-dimensional surface energy. To connect with the well-known literature on thin-plate theory, we employ the Föppl–von Kármán energy both for ease of interpretation as an effective model, and to exploit existing software developed for simulating thin elastic sheets (26).

The Föppl–von Kármán energy, which includes bending and stretching terms for a thin elastic sheet, can be written in terms of the first and second fundamental forms a and b of a flat region $\Omega \in \mathbb{R}^2$ mapped to the three-dimensional midsurface of the sheet in $\mathbb{R}^3$:

$$U = \frac{1}{2}\int_\Omega \left[\frac{h}{4}\left\|a_0^{-1}(a-a_0)\right\|_e^2 + \frac{h^3}{12}\left\|a_0^{-1}(b-b_0)\right\|_e^2\right] dA, \quad [1]$$

where the norm $\|X\|_e^2 = \frac{Y\nu}{1-\nu^2}\mathrm{tr}^2 X + \frac{Y}{1+\nu}\mathrm{tr}(X^2)$, a_0 and b_0 represent the initial (zero-energy) fundamental forms of the sheet, and Young's modulus and Poisson ratio are Y and ν respectively. In this formulation, the Young's modulus becomes a constant factor in the total energy and its value does not affect the minimum energy surface geometry. For flat sheets with no internal stresses, $a_0 = I$ and $b_0 = 0$; for sheets with flat metric but with natural curvatures κ_x and κ_y in the x and y directions respectively, $b_0 = -\mathrm{diag}\left(\kappa_x, \kappa_y\right)$, a diagonal matrix. For a triangular mesh approximating a continuous surface, the integral is replaced by a sum over triangles. We discretize the surface by first subdividing the mesh into rectangles with horizontal and vertical dimensions corresponding to those of a knitted stitch; we then subdivide each rectangle with an unstructured triangle mesh. Simulations in Fig. 3 contain between 100,000 and 400,000 triangles per mesh. To compute the energy, we follow the finite-difference scheme used in ref. 26 to define a_t and b_t on triangle t as

$$a_t = \begin{pmatrix} \vec{e}_1\cdot\vec{e}_1 & \vec{e}_1\cdot\vec{e}_2 \\ \vec{e}_1\cdot\vec{e}_2 & \vec{e}_2\cdot\vec{e}_2 \end{pmatrix}, \quad b_t = \begin{pmatrix} 2\vec{e}_1\cdot\Delta\vec{n}_{20} & -2\vec{e}_1\cdot\vec{n}_0 \\ -2\vec{e}_1\cdot\vec{n}_0 & 2\vec{e}_2\cdot\Delta\vec{n}_{01} \end{pmatrix} \quad [2]$$

with $\vec{e}_i$ as the directed edges of the triangle, $\vec{n}_i$ as the surface normals, and $\Delta\vec{n}_{ij} = \vec{n}_j - \vec{n}_i$. Surface normals are defined on the midpoint of and constrained to be perpendicular to each edge in the mesh, which requires one extra degree of freedom per edge of the mesh and is detailed in ref. 27. With these definitions of a and b, the total area-weighted Föppl–von Kármán energy of all triangles is minimized over the mesh degrees of freedom (the free vertex positions and edge normals) using the L-BFGS method. Code is available at https://github.com/jeffersontide/knitogami2024.

Data, Materials, and Software Availability. Code data have been deposited in GitHub (https://github.com/jeffersontide/knitogami2024). All study data are included in the main text.

ACKNOWLEDGMENTS. We thank Chelsea E. Amanatides for her extensive work in the initial conception of this project, as well as fabrication of all physical samples. We also thank Michael S. Dimitriyev and an anonymous reviewer for helpful comments on a draft of this paper. This work was supported by a Simons Investigator Grant from the Simons Foundation (R.D.K.) and the Kaufman Foundation New Research Initiative award. Effort was also sponsored by the U.S. Government under Other Transaction number HQ00342190016 between Advanced Functional Fabrics of America, Inc. and the Government. The U.S. Government and Advanced Functional Fabrics Of America (AFFOA) is authorized to reproduce and distribute reprints for Governmental purposes

notwithstanding any copyright notation thereon. The views and conclusions contained herein are those of the authors and should not be interpreted as necessarily representing the official policies or endorsements, either expressed or implied, of the U.S. Government or AFFOA. Additionally, this material is based on research sponsored by Air Force Research Laboratory under Agreement Number FA8650-20-2-5506, as conducted through the flexible hybrid electronics manufacturing innovation institute, NextFlex, in support of U.S. Army Combat Capabilities Development Command (DEVCOM)–Soldier Center. The U.S. Government is authorized to reproduce and distribute reprints for Governmental Purposes notwithstanding any copyright notation thereon. The views and conclusions contained herein are those of the authors and should not be interpreted as necessarily representing the official policies or endorsements, either expressed or implied, of Air Force Research Laboratory, the U.S. Army DEVCOM–Soldier Center or the U.S. Government.

1. I. Newton, *Philosophiæ naturalis principia mathematica* (The Royal Society of London, 1687).
2. W. Thomson, On the division of space with minimum partitional area. *Lond. Edinb. Dublin Philos. Mag. J. Sci.* **24**, 503–514 (1887).
3. J. C. Maxwell, On the cyclide. *Q. J. Pure Appl. Math.* **34**, 144–159 (1867).
4. C. W. Misner, K. S. Thorne, J. A. Wheeler, *Gravitation* (Macmillan, 1973).
5. R. J. Lang, *Origami Design Secrets: Mathematical Methods for an Ancient Art* (CRC Press, 2012).
6. A Yoshizawa, *Akira Yoshizawa: Japan's Greatest Origami Master* (Tuttle Publishing, 2016).
7. E. Demaine, T. Tachi, "Origamizer: A practical algorithm for folding any polyhedron" *in 33rd International Symposium on Computational Geometry (SoCG)*, B. Aronov, M. J. Katz, Eds. (Dagsthuhl Publishing, Germany, 2017), pp. 1–34.
8. Y. Klein, E. Efrati, E. Sharon, Shaping of elastic sheets by prescription of non-euclidean metrics. *Science* **315**, 1116–1120 (2007).
9. E. Siéfert, E. Reyssat, J. Bico, B. Roman, Programming stiff inflatable shells from planar patterned fabrics. *Soft Matter* **16**, 7898–7903 (2020).
10. D. Rant, A. Pavko-Cuden, *Foldable Weft Knitted Structures with Auxetic Potential* (Textiles of the Future: ISKA, 2013).
11. A. Pavko-Čuden, D. Rant, "Multifunctional foldable knitted structures: Fundamentals, advances and Applications" *in Textiles for Advanced Applications*, B. Kumar, S. Thakur, Eds. (IntechOpen, 2017), pp. 55–84.
12. S. Poincloux, M. Adda-Bedia, F. Lechenault, Geometry and elasticity of a knitted fabric. *Phys. Rev. X* **8**, 021075 (2018).
13. C. Amanatides, O. Ghita, K. E. Evans, G. Dion, Characterizing and predicting the self-folding behavior of weft-knit fabrics. *Text. Res. J.* **92**, 4060–4076 (2022).
14. K. Singal *et al.*, Programming mechanics in knitted materials, stitch by stitch. *Nat. Commun.* **15**, 2622 (2024).
15. A. Kurbak, O. Ekmen, Basic studies for modeling complex weft knitted fabric structures part I: A geometrical model for widthwise curlings of plain knitted fabrics. *Text. Res. J.* **78**, 198–208 (2008).
16. J. M. Kaldor, D. L. James, S. Marschner, "Simulating knitted cloth at the yarn level" in *ACM SIGGRAPH 2008 papers* (Association for Computing Machinery, 2008), pp. 1–9.
17. A. A. Jeddi, Z. Khorram-Toussi, V. Maleki, K. Yazdanifar, Relations between fabric structure and friction: Part II: Weft knitted fabrics. *J. Text. Inst.* **95**, 359–367 (2004).
18. R. Bai *et al.*, Experimental study of yarn friction slip and fabric shear deformation in yarn pull-out test. *Compos. Part A Appl. Sci. Manuf.* **107**, 529–535 (2018).
19. S. Poincloux, M. Adda-Bedia, F. Lechenault, Crackling dynamics in the mechanical response of knitted fabrics. *Phys. Rev. Lett.* **121**, 058002 (2018).
20. M. Popescu, M. Rippmann, T. Van Mele, P. Block, "Automated generation of knit patterns for non-developable surfaces" in *Humanizing Digital Reality: Design Modelling Symposium Paris 2017*, K. De Rycke *et al.*, Eds (Springer, 2018), pp. 271–284.
21. V. Narayanan, L. Albaugh, J. Hodgins, S. Coros, J. Mccann, Automatic machine knitting of 3D meshes. *ACM Trans. Graph.* **37**, 1–15 (2018).
22. G. Dion, "Knitogami 1 2" *in Bridges 2024 Exhibition of Mathematical Art, Craft, and Design (2024).* https://gallery.bridgesmathart.org/exhibitions/bridges-2024-exhibition-of-mathematical-art/genevieve-dion. Accessed 14 January 2025.
23. K. Luan, A. West, E. DenHartog, M. McCord, Auxetic deformation of the weft-knitted miura-ori fold. *Text. Res. J.* **90**, 617–630 (2020).
24. X. Ruan, T. W. Chou, Experimental and theoretical studies of the elastic behavior of knitted-fabric composites. *Compos. Sci. Technol.* **56**, 1391–1403 (1996).
25. K. O. Anwar *et al.*, "The effect of architecture on the mechanical properties of knitted composites" in *Proceedings of the 11th International Conference on Composite Materials: Textile Composites and Characterisation*, M. L. Scott, Ed. (Woodhead Publishing, 1997), vol. 5, p. 328.
26. W. M. van Rees, E. Vouga, L. Mahadevan, Growth patterns for shape-shifting elastic bilayers. *Proc. Natl. Acad. Sci. U.S.A.* **114**, 11597–11602 (2017).
27. C. Weischedel, "A discrete geometric view on shear-deformable shell models," PhD thesis, Georg-August-Universität, Göttingen (2012).